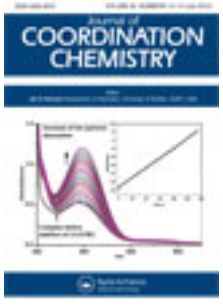

Journal of Coordination Chemistry
Publication details, including instructions for authors and subscription information:
http://www.tandfonline.com/loi/gcoo20

Structural and catalytic aspects of copper(II) complexes containing 2,6-bis(imino)pyridyl ligands

S.Y. Shaban [a b], A.M. Ramadan [a] & R. van Eldik [b]

[a] Chemistry Department, Faculty of Science, Kafrelsheikh University, Kafrelsheikh, Egypt

[b] Department of Chemistry and Pharmacy, University of Erlangen-Nuremberg, Egerlandsr. 1, 91058 Erlangen, Germany

Accepted author version posted online: 29 May 2012.Published online: 13 Jun 2012.

To cite this article: S.Y. Shaban, A.M. Ramadan & R. van Eldik (2012) Structural and catalytic aspects of copper(II) complexes containing 2,6-bis(imino)pyridyl ligands, Journal of Coordination Chemistry, 65:14, 2415-2431, DOI: 10.1080/00958972.2012.695017

To link to this article: http://dx.doi.org/10.1080/00958972.2012.695017

Journal of Coordination Chemistry
Vol. 65, No. 14, 20 July 2012, 2415–2431

Structural and catalytic aspects of copper(II) complexes containing 2,6-bis(imino)pyridyl ligands

S.Y. SHABAN*†‡, A.M. RAMADAN† and R. VAN ELDIK*‡

†Chemistry Department, Faculty of Science, Kafrelsheikh University, Kafrelsheikh, Egypt
‡Department of Chemistry and Pharmacy, University of Erlangen-Nuremberg, Egerlandsr. 1, 91058 Erlangen, Germany

(*Received 24 February 2012; in final form 26 April 2012*)

The synthesis, structure, and ligand substitution mechanism of a new five-coordinate trigonal-bipyramidal copper(II) complex, $[Cu^{II}(py^{t}BuMe_2N_3)Cl_2]$ (**1**), with a sterically constrained $py^{t}BuMe_2N_3$ chelate ligand, $py^{t}BuMe_2N_3 = 2,6\text{-}bis$-(ketimino)pyridyl, are reported. The kinetics and mechanism of chloride substitution by thiourea, as a function of nucleophile concentration, temperature, and pressure, were studied in detail and compared with an earlier study reported for the analogous complex $[Cu^{II}(py^{t}BuN_3)Cl_2]$ (**2**) $[py^{t}BuN_3 = 2,6\text{-}bis$-(aldimino)pyridyl]. Catalysis of the oxidation of 3,5-di-tert-butylcatechol to 3,5-di-tert-butylquinone by **1** and **2** was studied. Correlations between the reactivity, chloride substitution behavior, and reduction potentials of both complexes were made. These show that the rate of oxidation is independent of the rate of chloride substitution, indicating that the substitution of chloride by catechol as substrate occurs in a fast step. Spectral data show a non-linear relationship between the ability of the complexes to oxidize 3,5-DTBC and the Lewis acidity of their copper(II) centers. Electrochemical data demonstrate that the most effective complex **1** has a E^0 value that approaches the E^0 value of the natural tyrosinase enzyme.

Keywords: Biomimetics; Structure; Imine complexes; Catalysis; Copper(II); Catecholase

1. Introduction

Oxidation of organic substrates by molecular oxygen under mild conditions is of great interest for industrial and synthetic processes both from an economical and environmental point of view [1]. Although the reaction of organic compounds with oxygen is thermodynamically favored, it is kinetically hindered due to the triplet ground state of dioxygen. The synthesis and investigation of functional model complexes for metallo enzymes with oxidase or oxygenase activity is therefore promising for the development of new and efficient catalysts for oxidation reactions. Catechol oxidase belongs, like tyrosinase, to the polyphenol oxidases which oxidize phenolic compounds to the corresponding quinones in the presence of oxygen. This reaction is of importance in medical diagnosis for the determination of the hormonally active catecholamines

*Corresponding authors. Email: shaban.shaban@sci.kfs.edu.eg; vaneldik@chemie.uni-erlangen.de

ISSN 0095-8972 print/ISSN 1029-0389 online
http://dx.doi.org/10.1080/00958972.2012.695017

adrenaline, noradrenaline, and dopa [2]. For this reason studies on the coordination chemistry of copper(II) complexes with chelates incorporating pyridine and imine donors have been of significant interest in recent years due to their relevance to histidine coordinated copper proteins, such as blue copper proteins, hemocyanin, tyrosinase, and cytochrome *c* oxidase [3]. Also in the past decade, interest in the chemistry of imine-based ligand systems has been revitalized by the discovery that their complexes may act as supporting ligands for a variety of excellent catalysts with a range of applications [4]. The bis-imine pyridine ligand in particular has attracted considerable attention for its ability to provide unprecedented Ziegler–Natta catalysts based on late transition metals [4].

This study is a continuation of our work on the structure and mechanism of ligand substitution of copper complexes derived from sterically demanding conjugated bis-imine pyridines (figure 1). In the previous study [5], the crystal structure of $[Cu^{II}(py^{t}BuN_3)Cl_2]$ showed the complex to be a five-coordinate species with trigonal-bipyramidal geometry. The mechanism of the substitution of chloride in $[Cu^{II}(py^{t}BuN_3)Cl_2]$ by a series of thiourea derivatives was studied and showed that the mechanism is associative. To the best of our knowledge, only a few studies have been performed on the mechanism of substitution in five-coordinate copper(II) complexes and have shown the mechanism to be associative [6].

Most functional and structural models for metalloproteins have been prepared by variation of the substituent on the ligands in order to match the spectral properties of the metalloproteins [7]. For example, Gibson *et al.* [8] reported that a change in the ligand environment $[2,6\text{-}(ArNCR^1)_2C_5H_3]$ of the system resulted in changes in catalyst productivity and polymer molecular weight. Changing the substituent on the imine functional group from a ketimine ($R^1 = CH_3$) to an aldimine ($R^1 = H$) resulted in differences in productivity, molecular weight, and molecular weight distribution. It was found to be advantageous to change the substituent on the imine functional group from aldimine to ketimine, i.e., by using diacetylpyridine instead of diformylpyridine, and to study the effect of methyl substituents on the electronic properties, ligand substitution mechanism, and biomimetic catecholase activity. We report here a detailed mechanistic study of the ligand substitution reactions of $[Cu^{II}(py^{t}BuMe_2N_3)Cl_2]$ in methanol as a function of the entering nucleophile concentration, temperature, and pressure. This study also focuses on a detailed mechanistic analysis of the oxidation of 3,5-di-*tert*-butylcatechol (3,5-DTBC) and the catecholase activity of the studied complexes.

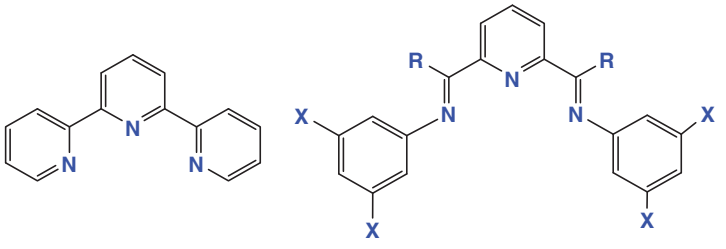

Terpy $\mathbf{L}^1$, R = CH^3; $\mathbf{L}^2$, R = H; X = *tert*-butyl

Figure 1. Schematic structure and abbreviations for ligands analogous to terpyridine.

In addition, electrochemical data were obtained in an attempt to correlate the reduction potentials with the reactivity of the complexes.

2. Experimental

2.1. *General*

2,6-Diacetylpyridine was purchased from Aldrich Chemical Co. and 2,6-di-*tert*-butylaniline was synthesized as described in the literature [5]. All other chemicals were obtained commercially and used as received unless stated otherwise.

2.2. *Instrumentation and measurements*

Spectra were recorded on the following instruments: IR (KBr discs, solvent bands were compensated): Mattson Infinity instrument (60 AR) at 4 cm^{-1} resolution from 400 to 4000 cm^{-1}; NMR: Jeol-JNM-GX 270, EX 270, and Lambda LA 400 with the protio-solvent signal used as an internal reference. Mass spectra: Jeol MSTATION 700 spectrometer; Elemental analyses: Carlo Erba EA 1106 or 1108 analyzer. Cyclic voltammetry measurements were performed in a one-compartment three-electrode cell using a gold working electrode (Metrohm) with a geometrical surface of 0.7 cm^2 connected to a silver wire pseudo-reference electrode and a platinum wire serving as counter electrode (Metrohm). Measurements were recorded with an Autolab PGSTAT 30 unit at room temperature. The working electrode surface was cleaned using 0.05 μm alumina, sonicated, and washed with water every time before use. The working volume of 10 mL was de-aerated by passing a stream of high purity N_2 through the solution for 15 min prior to the measurements and then maintaining an inert atmosphere of N_2 over the solution during the measurements. All CVs were recorded for the reaction mixture with a sweep rate of 50 mV s^{-1} at 25°C. Potentials were measured in 0.1 mol L^{-1} TBAP electrolyte and are reported *versus* a Ag/AgCl electrode. Kinetic investigations of the substitution of the dichloro complex by thiourea or tetramethylthiourea were performed either in tandem cuvettes with a path length of 0.88 cm, thermally equilibrated at 23.0 ± 0.1°C before mixing, using a Varian Cary 1G spectrophotometer, or on an Applied Photophysics SX 18MV stopped-flow instrument (also thermostated at 23.0 ± 0.1°C) with an optical pathlength of 1 cm at 394 nm.

For experiments at elevated pressure up to 150 MPa, a laboratory-made high-pressure stopped flow instrument was used for fast kinetic measurements [9], whereas a Shimadzu spectrophotometer equipped with a high pressure cell, combined with a pill-box optical cell, was used for slow kinetic measurements [10]. The temperatures of the instruments were controlled with an accuracy of ± 0.1°C. Thiourea was selected as entering nucleophile since its high nucleophilicity prevents back reaction with chloride. LiCl solutions (0.002 mol L^{-1}) were used to avoid spontaneous solvolysis of the chloro complexes. The ligand substitution reactions were studied under pseudo-first-order conditions by using at least a 10-fold excess of thiourea. All listed rate constants represent an average of at least three kinetic runs under each experimental condition.

2.3. *Catecholase biomimetic catalytic activity*

The catecholase catalytic activities of the copper(II) complexes (1 mmol L^{-1} in 25 mL methanol) were performed for the oxidation of catechol at room temperature, under atmospheric air as well as under inert atmosphere (N_2), where the electronic spectra were recorded at different time intervals. The oxidation of catechol was detected by spectrophotometric monitoring the appearance of *o*-quinone at 400 nm.

2.4. *Synthesis*

2.4.1. Synthesis of 2,6-diacetylpyridinebis(3,5-di-tert-butylanil) (L^1). 2,6-Diacetylpyridine (0.135 g, 1.0 mmol) and 3,5-di-*tert*-butylaniline (0.410 g, 2.0 mmol) were stirred in methanol (25 mL) for 6 h in the course of which a yellow solid was formed. The solid was filtered off, washed with cold methanol, and dried in vacuum to give **1**·CH_3OH in 96% yield. Anal. Calcd for $C_{38}H_{55}N_3O$ (%): C, 80.09; H, 9.73; N, 7.37. Found (%): C, 80.01; H, 9.46; N, 8.52. ^{1}H NMR ($CDCl_3$, 400 MHz): δ, ppm 8.76 (s, 2H, HC=N), 8.35 (d, $J=7.5$, 2H, $H_{\beta\ \text{pyridine}}$), 7.85 (t, $J=7.2$, 1H, $H_{\gamma\ \text{pyridine}}$), 7.25 (s, 2H, H_{arom}), 7.15 (s, 4H, H_{arom}), 2.43 (s, 6H, $2CH_3$), 1.33 (s, 36H, $(C(CH_3)_3)$). ^{13}C NMR ($CDCl_3$, 100 MHz): δ, ppm 167.2, 156.3, 152.1, 151.1, 137.2, 122.2, 119.2, 118.9, (C_{arom}), 114.3 (CH=N), 35.0 (CH_3), 32.1 ($C(CH_3)_3$), 16.5 ($C(CH_3)_3$). IR (KBr): ν, cm^{-1} 3062 (s, C–H_{arom}), 2962 (s, C–H_{aliph}), 1626 (m, C=N), 1595, 1585, 1523 (s, C=C_{arom}). MS (FD^+, EtOH): $m/z=538$ $[M]^+$.

2.4.2. Synthesis of 2,6-diacetylpyridinebis(3,5-di-tert-butylanil)$CuCl_2$ [Cu(py$Me_2^tBuN_3$)Cl_2] (1). $CuCl_2\cdot 2H_2O$ (0.511 g, 0.3 mmol) was added to a suspension of 2,6-bis(3,5-di-*tert*-butylphenylimino-1-ethyl)pyridine (L^1) (1.53 g, 0.3 mmol) in methanol and the mixture was stirred for 5 h. The resultant orange-brown product was filtered off, washed with cold methanol (5 mL), and dried in vacuum to give **1**.CH_3OH in 75% yield. Anal. Calcd for $C_{39}H_{59}Cl_2CuN_3O_2$ (734.33) (%): C, 63.61; H, 8.08; N, 5.71. Found (%): C, 63.32; H, 7.21; N, 5.75. IR (KBr): ν, cm^{-1} 3070 (s, C–H_{arom}), 2960, 2904 (s, C–H_{aliph}), 1650 (m, C=N). MS (FD^+, CH_3OH): $m/z=675$ $[M]^+$.

3. Results and discussion

3.1. *Synthesis and characterization*

2,6-*Bis*-(ketimino)pyridine, L^1, was synthesized in high yield *via* Schiff-base condensation of one equivalent of 2,6-diacetylpyridine with two equivalents of 3,5-di-*tert*-butylaniline. L^1 behaves as a neutral tridentate chelating agent and its copper(II) complex, **1**, was synthesized by treating with $CuCl_2$ in methanol (scheme 1). FAB mass spectrum and microanalysis of **1** confirmed the suggested formula $[Cu^{II}(py^tBuMe_2N_3)Cl_2]$. The azomethine band ν(C=N) in **1** undergoes a remarkable shift to higher wavenumbers as a result of coordination of the nitrogen to the metal ion [11]. The in-plane ring deformation band δ(py) at 585–624 cm^{-1} in the spectrum of the

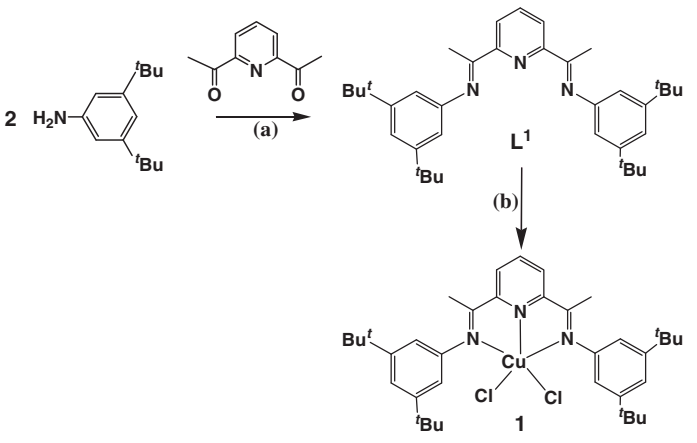

Scheme 1. Synthesis of $\mathbf{L^1}$ and its copper(II) complex **1**; (a) MeOH, 65°C, 10 h; (b) $CuCl_2$, MeOH, 65°C, 7 h.

free ligand is shifted 612–650 upon complexation due to bonding through the pyridyl nitrogen [12].

Due to the lack of an X-ray structure of the reported copper(II) complex $[Cu^{II}(py^tBuMe_2N_3)Cl_2]$ (**1**), comparative spectral and magnetic investigations were carried out with the related copper(II) complex $[Cu^{II}(py^tBuN_3)Cl_2]$ (**2**) [5]. X-ray structural analysis demonstrated that **2** consists of a five-coordinate trigonal bipyramidal copper(II) [5]. The room temperature magnetic moments of **1** and **2** in the solid state, 1.9 and 1.88 BM, respectively, are consistent with the formulation of the complexes as copper(II) monomers with one unpaired electron. The spectra of both complexes in methanol exhibit broad asymmetric absorption bands at ~720 nm ($\epsilon = 1200\,L\,mol^{-1}\,cm^{-1}$), which are in the range expected for the d–d transition of the tetragonal distorted copper(II) complex [13]. In addition, a strong absorption in the low energy region can be assigned to the $n \rightarrow \pi^*$ transition that originates from the azomethine linkage of the imine moiety of the ligand [14].

The position and intensity of this band depends on the type of substituent within the carbonyl moiety of the Schiff-base ligands. The increasing energy of this band from **1** to **2** (figure 2) reflects the decreasing order of the Lewis acidity of the copper(II) center [11]. The presence of the electron-donating group (CH_3) in $\mathbf{L^1}$ shifts the $n \rightarrow \pi^*$ band of C=N to higher energy compared to the hydrogen in $\mathbf{L^2}$.

The X-band ESR spectra of **1** and **2** were measured at room temperature. The spectral features are similar and exhibit intense ESR signals that are characteristic of the rhombic symmetry with three g-values. The observed g-values (g_1, g_2, and g_3 in the order of decreasing magnitude) were computed from the spectra using DPPH ($g = 2.0023$) as g marker. In the rhombic symmetry, all orbital degeneracy must disappear. The presence of a relatively weak rhombic distortion is apparent in the splitting of the perpendicular resonance into two closely spaced components (g_2 and g_3) in all cases. For the five-coordinate copper(II) complexes the probable configurations, namely square pyramidal and trigonal bipyramidal, are characterized by the ground-state $d_{x^2-y^2}$ and d_{z^2} orbitals, respectively. ESR spectra for the five-coordinate copper(lI) complexes provide a very good basis for distinguishing between these two states. For systems with $g_1 > g_2 > g_3$, the ratio of $(g_2 - g_3)/(g_1 - g_2) = R$ is very useful. If the ground

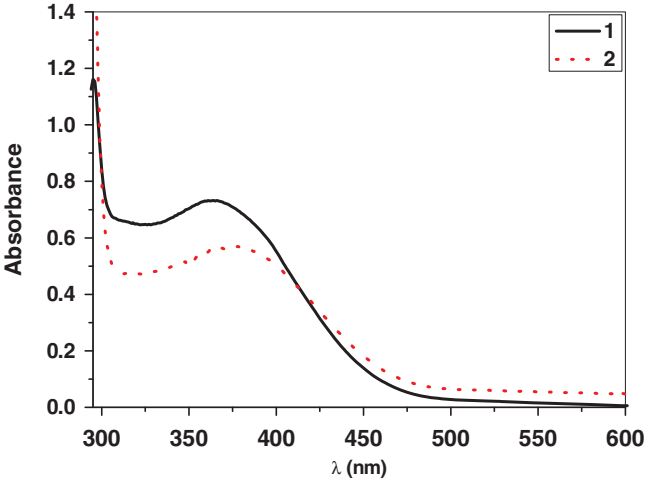

Figure 2. UV-Vis spectra recorded for **1** (—) and **2** (···) (0.5×10^{-4} mol L^{-1}) in methanol at 296 K.

state is d_{z^2} the value of R is larger than 1. On the other hand, if the ground state is $d_{x^2-y^2}$ the value of R is less than 1 [11]. The five-coordinate copper(II) complexes under study show values of R larger than 1, thus indicating a five-coordinate trigonal bipyramidal geometry. On the basis of these arguments, a five-coordinate trigonal bipyramidal structure may be assigned for **1**.

The electrochemical behavior of **1** was studied and compared with that of **2** to provide more information on the nature of the complex in solution. Cyclic voltammograms were recorded in MeOH *versus* a Ag/Ag^+ reference electrode (figure 3). In contrast to the analogous complex **2**, compound **1** exhibits only one peak. One-electron oxidation occurs at 0.51 V and the corresponding reduction at 0.38 V. The peak at 0.51 V has the typical symmetrical shape of an adsorption phenomenon. This may explain the i_{pa}/i_{pc} value > 1. The relatively high ΔE_p value of 126 mV may suggest that a E_{qrev} or E_{irrev} electrochemical mechanism is operating (i.e., slow electron transfer related to heavy structural reorganization after the electron transfer, without chemical complications) [15]. On the basis of the former data, the overall redox process may simply be the chemically reversible, but electrochemically quasi-reversible and adsorption-complicated Cu(II)/Cu(I) reduction [16]. The effect of chlorides (added as LiCl) may simply be to interfere with this adsorption, "cleaning" the diffusion peak below.

A comparison of **1** with that found for the analogous $[Cu^{II}(py^tBuN_3)Cl_2]$ complex indicates that the introduction of two methyl substituents into the bis-imine moiety shifts $E_{1/2}$ to a more positive value (from 44 mV for **1** to 70 mV for **2**). An explanation for this is most likely related to electron donation of the methyl substituent that leads to an increase in the electron density on the metal center.

3.2. *Kinetic studies on ligand substitution*

Previous studies on copper(II) catecholase functional models demonstrated that the exchange interaction between the catecholase anion radical with a good leaving group

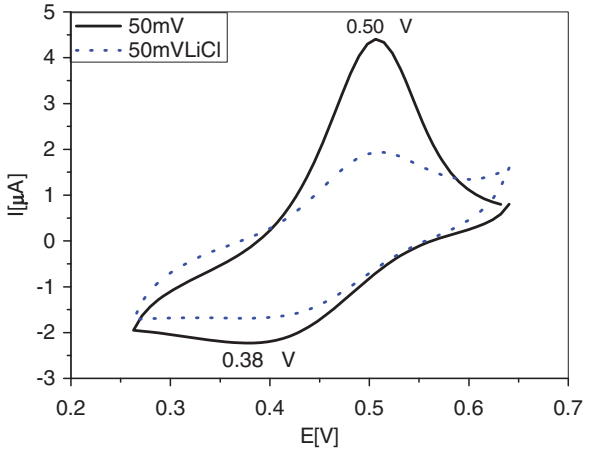

Figure 3. (a) Cyclic voltammograms of $[Cu^{II}(py^{t}BuMe_2N_3)Cl_2]$ (**1**) (— before and - - - after addition of $0.1\,mol\,L^{-1}$ LiCl). Measurements were performed on a Pt working electrode *vs.* a non-aqueous Ag/Ag^+ reference electrode; add 544 mV [300 mV, Ag/Ag^+ to SCE; +244 mV, SCE to SHE] to convert to standard hydrogen electrode (SHE); Fc/Fc^+ couple in CH_3CN, $E_{½}$, 0.414 V (CV); supporting electrolyte $0.1\,mol\,L^{-1}$ NBu_4PF_6, scan rate = $50\,mV\,s^{-1}$, potentials given in V, complex concentration $0.2\,mmol\,L^{-1}$.

incorporated in the complex initiates the catalytic oxidation cycle. If the coordinating groups are stronger ligands than the catecholate, no oxidation will be observed for the five-coordinate copper(II) catecholase models. To further elucidate the biomimetic catalytic activity of the reported copper(II) catecholase models **1** and **2**, a detailed kinetic study on chloride substitution of **1** was carried out and compared with that for **2**. Thiourea was selected as entering nucleophile because of its high nucleophilicity that will prevent back reaction with chloride. Furthermore, it was selected as a neutral entering ligand such that the overall reaction is accompanied by charge creation, and the formation of the transition state may involve changes in dipole moment [5, 17].

Reactions of **1** with thiourea can be monitored kinetically in the range of *ca* 360–400 nm. Solutions were prepared by dissolving known amounts of **1** in methanol in the presence of $0.002\,mol\,L^{-1}$ LiCl to prevent the spontaneous solvolysis reaction. The substitution reactions were studied as a function of TU concentration, temperature, and pressure in methanol. Figures 4 and 5 show UV-Vis spectral changes and representative kinetic traces, respectively.

Rate constants for the reactions were determined by using total TU concentrations of $0.001-0.25\,mol\,L^{-1}$, i.e., always at least in 10-fold excess over the Cu(II) complex. Throughout the nucleophile concentration range it was possible to fit the absorbance/time traces to a two-exponential function by using the following equation:

$$A = a_1 e^{-k_{obsd1}t} + a_2 e^{-k_{obsd2}t} + A_0 \quad (1)$$

The overall reaction is biphasic and in line with that reported for **2**. An initial fast reaction (rate constant k_{obsd1}) is followed by a much slower one (rate constant k_{obsd2}). k_{obsd1} increases linearly with TU concentration (figure 6), which leads to the second-order rate constant $k_1 = 3.6 \pm 0.1\,(mol\,L^{-1})^{-1}\,s^{-1}$. Rate constant k_{obsd2} also depends linearly on the TU concentration with second-order rate constant $k_2 = (3.8 \pm 1.1) \times 10^{-2}\,(mol\,L^{-1})^{-1}\,s^{-1}$ (figure 6). The rate constants demonstrate that

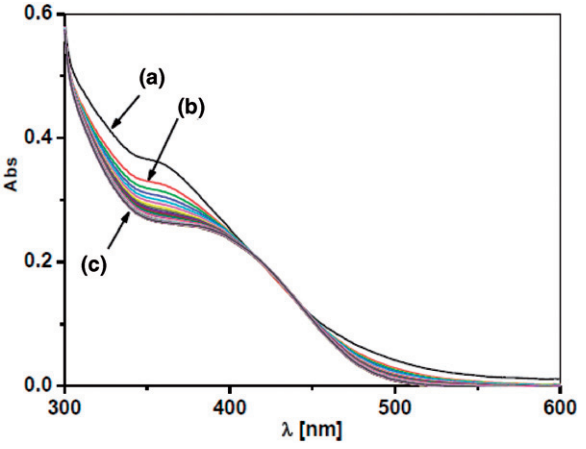

Figure 4. UV-Vis spectral changes recorded for the reaction of **1** (0.5×10^{-4} mol L^{-1}) with thiourea (250 mmol L^{-1}) in methanol at 296 K: (a) spectrum before the reaction; (b) spectrum obtained a few seconds after mixing of the reactants; (c) spectrum obtained after 100 min.

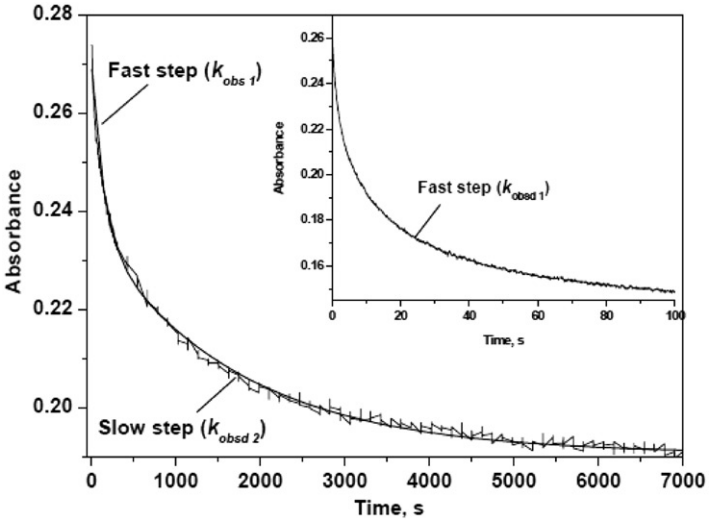

Figure 5. Absorbance-time traces at 350 nm for the reaction of **1** (0.5×10^{-4} mol L^{-1}) with thiourea (250 mmol L^{-1}) in methanol at 296 K (solid line obtained by fitting the data with a double exponential function according to equation (1)). The inset represents the kinetic trace of the fast reaction measured by stopped-flow instrument.

the second substitution is slowed by two orders of magnitude due to the displacement of one chloride by thiourea.

The observed kinetic behavior can be accounted for in terms of two subsequent substitution reactions (equation (2)) in which the two chlorides are sequentially displaced by TU characterized by the second-order rate constants k_1 and k_2, respectively.

$$\left[\mathrm{Cu(L)(Cl)_2}\right]^0 \xrightarrow[k_1]{\mathrm{TU}} \left[\mathrm{Cu(L)(Cl)TU}\right]^+ \xrightarrow[k_2]{\mathrm{TU}} \left[\mathrm{Cu(L)(TU)_2}\right]^{2+} \quad (2)$$

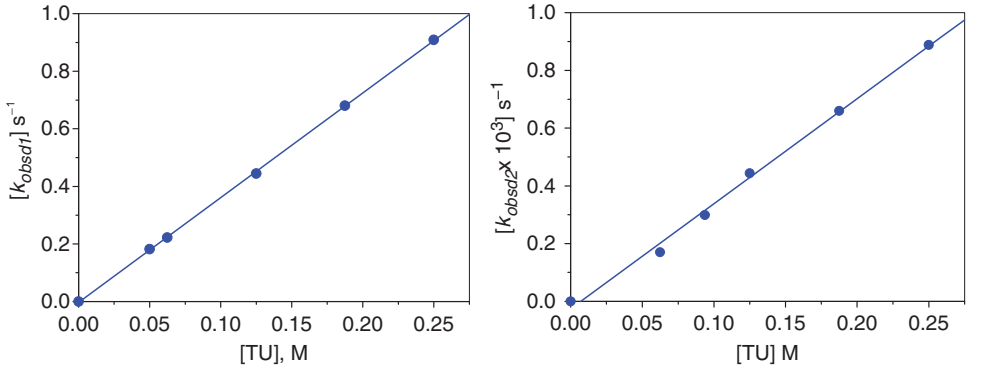

Figure 6. Plots of k_{obsd} *vs.* thiourea concentration for **1** in methanol at 296 K (left: first reaction step; right: second reaction step). Experimental conditions: $[\mathbf{1}] = 0.5 \times 10^{-4}$ mol L^{-1}, 0.002 mol L^{-1} LiCl.

Table 1. Summary of the rate and activation parameters for the substitution of the chloride ligands in $[Cu^{II}(py^tBuMe_2N_3)Cl_2]$ (**1**) and $[Cu^{II}(py^tBuN_3)Cl_2]$ (**2**) by TU in methanol in the presence of 2 mmol L^{-1} LiCl.

Complex		k^{296} ((mol L^{-1})$^{-1}$ s^{-1})	$\Delta H^{\#}$ (kJ mol^{-1})	$\Delta S^{\#}$ (JK^{-1} mol^{-1})	$\Delta V^{\#}$ (cm^3 mol^{-1})
1	First step	3.6 ± 0.1	40 ± 1	-100 ± 5	-14.0 ± 0.3
	Second step	$(3.8 \pm 1.1) \times 10^{-2}$	35.6 ± 0.8	-172 ± 3	-19.3 ± 0.6
2[a]	First step	918 ± 30	42 ± 2	-46 ± 7	-6.5 ± 0.2
	Second step	1.62 ± 0.06	58 ± 2	-47 ± 6	-5.3 ± 0.7

[a]Ref. [5].

It follows from this reaction scheme that k_{obs1} and k_{obs2} should depend linearly on the entering TU concentration in the absence of a back reaction as shown in figure 6, such that $k_{obs1} = k_1$[Nu] and $k_{obs2} = k_2$[Nu]. The rate constants in table 1 show that the second substitution reaction with thiourea is much slower than the first one. This can be ascribed to steric hindrance on the Cu(II) center caused by the displacement of chloride by thiourea. A comparison of k_1 and k_2 with that found for the analogous $[Cu^{II}(py^tBuN_3)Cl_2]$ complex indicates that the introduction of two methyl substituents on the bis-imine slows the first reaction 250 times and the second reaction 40 times at 296 K. A likely explanation for this decrease in rate is related to two factors: (i) the electron donation of the methyl substituents leads to an increase in the electron density at the metal center and hence a decrease in electrophilicity; (ii) the steric factor arising from the two methyl groups attached directly to the imine linkage limits the freedom of rotation of the aryl ring substituents [8, 18].

Since activation parameters such as $\Delta S^{\#}$ and $\Delta V^{\#}$ are sensitive probes that reflect the nature of the transition state of a given reaction, their determination serves as a useful mechanistic tool in assigning the mechanism of the TU substitution reaction. The temperature and pressure dependences of the substitution rate constants were studied by stopped-flow and spectrophotometric techniques from 12°C to 28°C (limited due to low solubility of the complex) and pressure range 10–150 MPa, respectively. The observed temperature and pressure dependencies are presented in figures 7 and 8, respectively, and the plots are linear over the ranges studied. From these plots the activation parameters for the TU substitution reaction were estimated, and the data are

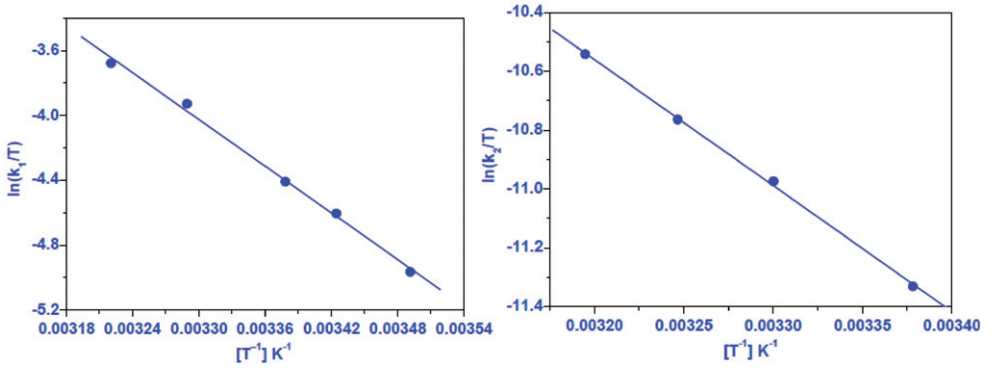

Figure 7. Temperature dependence of the reactions of **1** with thiourea in methanol (left, first reaction step; right: second reaction step). Experimental conditions: [**1**] = 0.5×10^{-4} mol L^{-1}, [TU] = 0.25 mol L^{-1}, 0.002 mol L^{-1} LiCl.

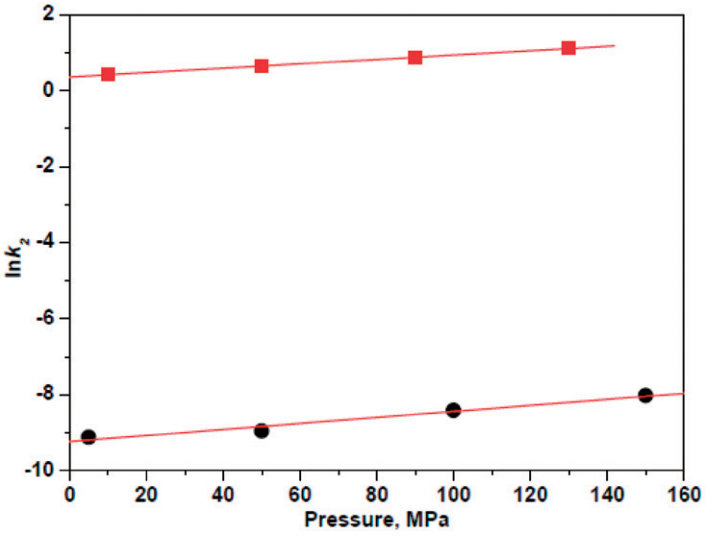

Figure 8. Pressure dependence of the reaction of **1** with thiourea in methanol (■ first reaction step, • second reaction step). Experimental conditions: [**1**] = 0.1 mmol L^{-1}, [TU] = 0.015 mol L^{-1}, 296 K, 0.002 mol L^{-1} LiCl.

summarized in table 1. The values of $\Delta S^{\#}$ and $\Delta V^{\#}$ are much more negative than those reported for [Cu^{II}(py^t*Bu*N$_3$)Cl$_2$], supporting an associative mechanism for both reaction steps in reaction (2) rather than an associative interchange (I_a) mechanism [19]. In this case, the transition state of the process is expected to have six-coordinate character on forming a bond between the five-coordinate Cu(II) complex and the entering nucleophile. The activation parameters reported in table 1 also support this suggestion.

3.3. *Kinetic studies on the reaction with 3,5-DTBC*

In most catecholase-like activity studies of synthetic model complexes, 3,5-DTBC has been employed as substrate. The product 3,5-di-*tert*-butyl-*o*-quinone (3,5-DTBQ) is

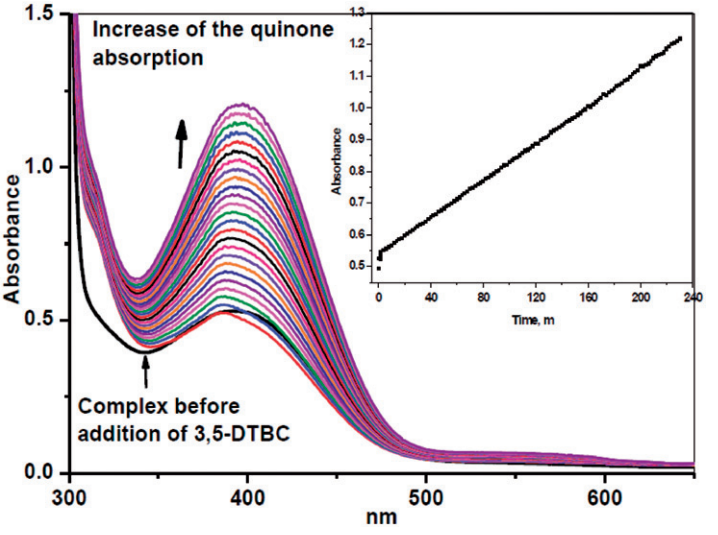

Figure 9. UV-Vis spectral changes recorded for the reaction of **1** (0.1 mmol L^{-1}) with 3,5- DTBC (100 mmol L^{-1}) in MeOH at 296 K. Inset shows the course of the absorbance at 400 nm with time (in minutes).

stable and has a strong absorption at $\lambda_{max} = 400$ nm [20]. Therefore, activities and reaction rates can be determined using electronic spectroscopy by following the appearance of the absorption maximum of the quinone. The reactivity studies were performed in methanol and THF solutions because of the good solubility of the complexes, the substrate (3,5-DTBC) and its product (3,5-DTBQ) in these solvents. Prior to a detailed kinetic study, it was first necessary to estimate approximately the ability of the complexes to oxidize catechol. For this purpose, 0.1 mmol L^{-1} solutions of **1** and **2** in methanol were treated with 100 mmol L^{-1} of 3,5-DTBC in the presence of air. The course of the reaction was followed by UV-Vis spectroscopy over the first 200 min. The results indicate that the reactivity of **1** is higher than that of **2**, and can be expressed in turnover numbers of 30 min^{-1} for **1** *versus* 12 min^{-1} for **2**. The course of the catecholase reaction with a solution of **1** is shown in figure 9 for the reaction in methanol.

It is clear from the results in figure 9 that the addition of 100 mmol L^{-1} of 3,5-DTBC to the complex has an immediate influence on the UV-Vis spectrum. The bands in the charge-transfer region as well as the d–d bands change with respect to position and intensity. Therefore, binding of 3,5-DTBC to copper(II) should be considered as the first rapid step. Due to the developing product bands in the UV-Vis spectrum of the complex, it is difficult to make a clear statement about the nature of the coordination of catechol to the metal center. We have therefore used stopped-flow techniques to study the rapid reaction with 3,5-DTBC in more detail. The complex spectrum changes dramatically upon the addition of 3,5-DTBC during the first 30 s, as shown in figure 10. The kinetics of this reaction could be followed at 400 nm. The kinetics of the subsequent slow reaction was studied by the initial rate method by monitoring the absorbance change at 400 nm (see inset in figure 9).

The same reaction in THF occurs orders of magnitude faster and the results in figure 11 show that the absorbance *versus* time plot at 400 nm after the addition of

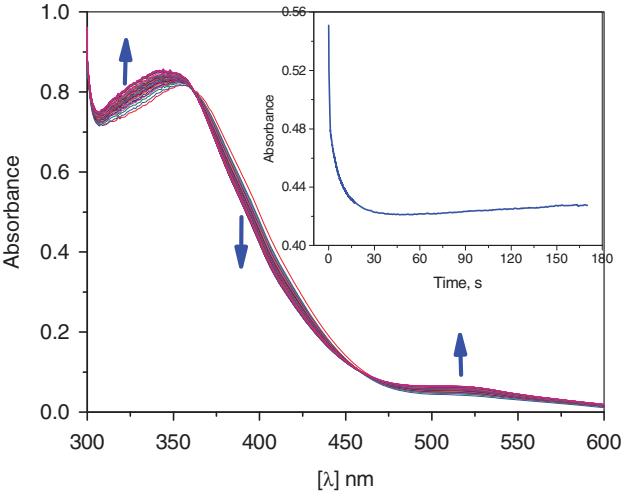

Figure 10. UV-Vis spectral changes recorded for the first reaction step of **1** ($0.1\,mmol\,L^{-1}$) with 3,5-DTBC ($18\,mmol\,L^{-1}$) in MeOH at 296 K. Inset: representative kinetic trace obtained by stopped-flow spectrophotometry monitored at 400 nm.

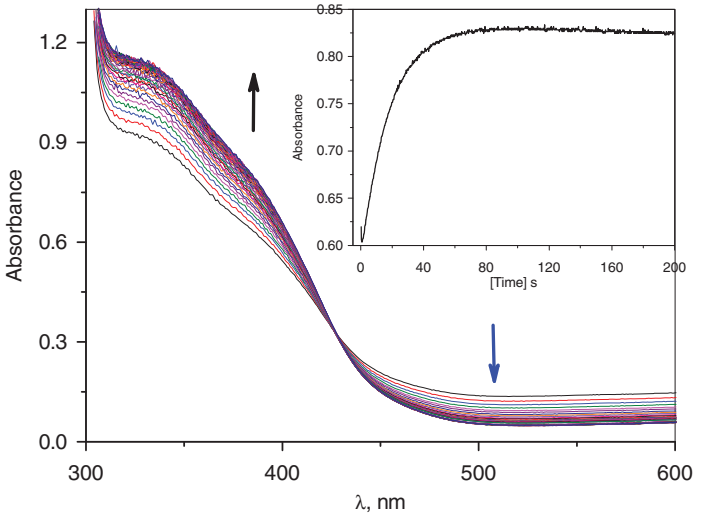

Figure 11. UV-Vis spectral changes recorded for the reaction of **1** ($0.5 \times 10^{-4}\,mol\,L^{-1}$) with 3,5- DTBC ($225\,mmol\,L^{-1}$) in THF at 296 K. Inset: kinetic trace of the overall reaction between 3,5-DTBC and **1** in THF monitored by stopped-flow spectrophotometry at 400 nm. Experimental points superimposed with the best single-exponential fit.

3,5-DTBC also proceeds in two steps, namely a fast decrease in absorbance in the first step followed by an increase in absorbance in the second step. The second step cannot be observed when the experiment is repeated under inert atmosphere (i.e., in the absence of oxygen), indicating that the growing band is due to quinone formation. More information on the first reaction step could be obtained from stopped-flow measurements over the first few seconds at 400 nm as shown in figure 12.

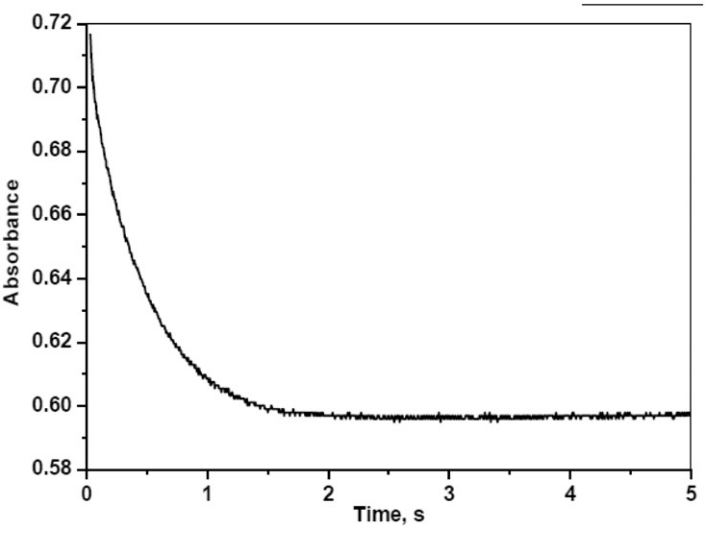

Figure 12. Representative kinetic trace for the first reaction step between 3,5-DTBC and **1** in THF obtained by stopped-flow spectrophotometry monitored at 400 nm. Experimental points superimposed with the best single-exponential fit. Conditions: $T = 296\,\mathrm{K}$; $[\mathbf{1}] = 0.5 \times 10^{-4}\,\mathrm{mol\,L^{-1}}$ and $[3,5\text{-DTBC}] = 75\,\mathrm{mmol\,L^{-1}}$.

To determine the dependence of the observed reactions on the substrate concentration, solutions of **1** were treated with different concentrations of 3,5-DTBC in both methanol and THF. For the first step, a first-order dependence on the substrate concentration was observed in both cases (figures 13 and 14). Thus, we propose a rapid pre-equilibrium involving adduct formation between the Cu(II) complex and 3,5-DTBC (equation (3)). The results obtained in both solvents show that the coordination affinity of 3,5-DTBC in THF ($K_1 = k_1/k_{-1} = 7.3\,(\mathrm{mol\,L^{-1}})^{-1}$) is smaller than in MeOH ($K_1 = k_1/k_{-1} = 11.3\,(\mathrm{mol\,L^{-1}})^{-1}$) (figures 13 and 14, respectively). The reason for this can be traced to the higher basicity of methanol which can assist in the deprotonation of 3,5-DTBC.

$$\mathrm{Cu^{II}\ complex} + \text{3,5-DTBC} \underset{k_{-1}}{\overset{k_1}{\rightleftharpoons}} \mathrm{Cu^{II}\text{-}DTBC\ adduct} \xrightarrow[k_2]{\mathrm{O_2}} \mathrm{Cu^{II}complex} + \mathrm{DTBQ} \quad (3)$$

For the second step of the reaction between 3,5-DTBC and **1** in methanol, a first-order dependence on the substrate concentration was observed at low concentrations of 3,5-DTBC. At higher substrate concentrations, saturation kinetics was observed (figure 15). The irreversible conversion into the quinone product is considered to be the rate-determining step, i.e., $k_2 \ll k_{-1}$ and $K_1 = k_1/k_{-1}$. Although a much more complicated mechanism may be involved, the results show that this simple model is sufficient for a kinetic description. The rate law for the reaction sequence in (3) is given by (4):

$$V = \frac{\mathrm{d[DTBQ]}}{\mathrm{d}t} = k_2\left[\mathrm{Cu^{II}complex - adduct}\right] = \frac{k_2 k_1\left[\mathrm{Cu^{II}complex}\right][3,5\text{-DTBC}]}{1 + k_1[3,5\text{-DTBC}]}$$

where V is the rate of product formation, which can be rewritten as

$$\frac{V}{\left[\mathrm{Cu^{II}complex}\right]} = \frac{k_2 k_1[3,5\text{-DTBC}]}{1 + k_1[3,5\text{-DTBC}]} \quad (4)$$

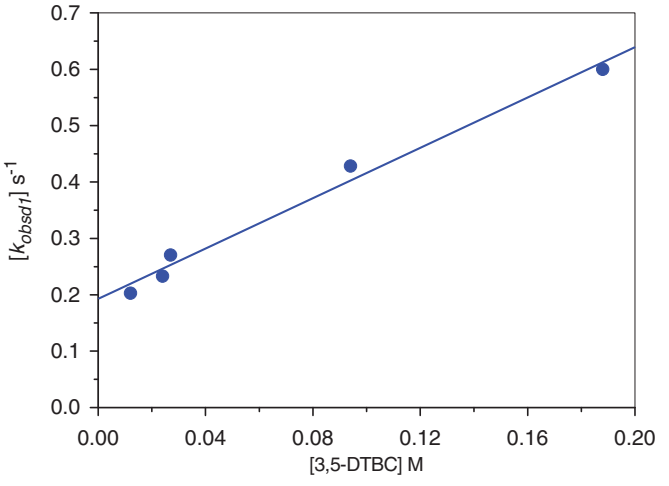

Figure 13. Plot of k_{obs1} *vs.* 3,5-DTBC concentration for the first reaction step between 3,5-DTBC and 0.5×10^{-4} mol L^{-1} **1** in MeOH at 296 K. The reaction was monitored at 400 nm ($K_1 = k_1/k_{-1} = 11.3\,(\text{mol L}^{-1})^{-1}$).

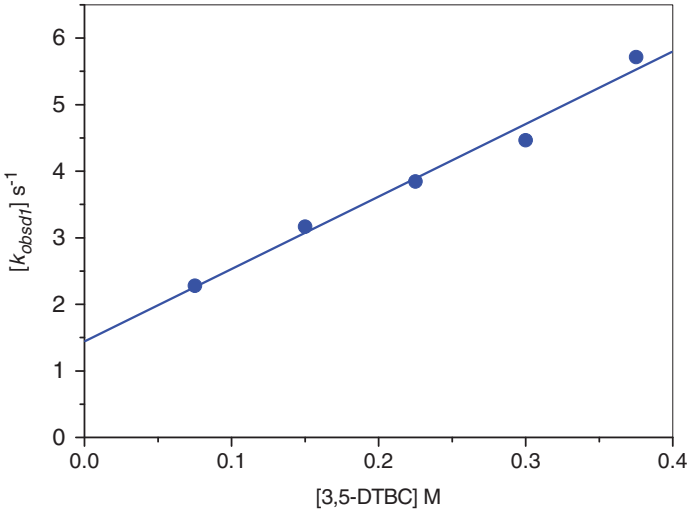

Figure 14. Plot of k_{obs1} *vs.* 3,5-DTBC concentration for the first reaction step between 3,5-DTBC and 0.5×10^{-4} mol L^{-1} **1** in THF at 296 K ($K_1 = k_1/k_{-1} = 7.3\,(\text{mol L}^{-1})^{-1}$).

The maximum rate constant, k_2, is reached when the catalyst is completely saturated with 3,5-DTBC, i.e., at high [3,5-DTBC]. At a $V/[\text{Cu}^{\text{II}}\text{complex}]$ value of $k_2/2$, the $[3,5\text{-DTBC}] = 1/k_1$, which according to figure 15 results in $k_1 \approx 10\,(\text{mol L}^{-1})^{-1}$ for the reaction in methanol. This value is indeed very close to that found for k_1 in figure 13 and illustrates the validity of the kinetic model.

The greater catalytic activity of **1** compared to **2** can be correlated with their redox potentials. It should be noted that the enzyme tyrosinase, which catalyzes the aerobic

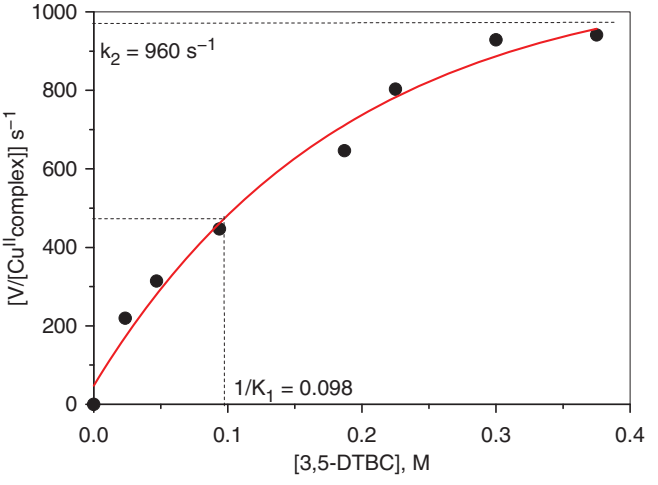

Figure 15. Dependence of the initial rate of the oxidation reaction of 3,5-DTBC on the concentration of the substrate 3,5-DTBC catalyzed by **1** in methanol. The concentration of **1** was 0.5×10^{-4} mol L^{-1} and the reaction was followed at 400 nm.

oxidation of catechol to the light absorbing *o*-quinone, has a reported E^0 value of 0.36 V *versus* the standard calomel reference electrode [8]. It is obvious, however, that the enzyme is able to balance successfully the requirements of the different oxidation states of the metal, $M^{n+} \rightleftharpoons M^{(n-1)+}$, in performing its catalytic tasks. The balance between the ease of reduction of copper(II) and subsequent re-oxidation of copper(I) by molecular oxygen must be maintained for efficient catalysis to occur. $E_{1/2}$ of **1** (0.44 mV) approaches the reported $E_{1/2}$ value of the natural enzyme whereas that of **2** (0.71 mV) is much higher [21, 22]. Several studies on catechol oxidation demonstrated that for five-coordinate copper(II) complexes with tetradentate ligands, the degree of lability of the fifth donor has an effect on the rate of catalysis [23]. In addition, it has been shown that electron transfer from catechol to copper(II) can begin only after catechol and the copper(II) species form a copper(II)-catecholate intermediate as suggested in reaction (3) [24]. Such an intermediate can easily be formed as mentioned above, which clearly showed that both **1** and **2** undergo associative ligand substitution reactions of the coordinated chloride ligands. The kinetic results showed that the order of lability of the coordinated chloride ligands is **1** < **2**, but the opposite order holds for their reaction with 3,5-DTBC. These results thus confirm that the catecholase mimetic activity is independent of either the rate of ligand displacement from the copper(II) complex or the difference in the dissociation constants for the loss of the chloride ligand. This suggests that displacement of chloride by catechol as substrate must be involved in a rapid pre-equilibrium step of the overall reaction sequence outlined in (3).

4. Conclusion

A new sterically constrained N_3 donor $\mathbf{L^1}$ was synthesized with the aim to understand the effect of ligand substituents in terms of electronic and steric factors on the structure,

spectral behavior and consequently the catecholase biomimetic catalytic activity of its copper(II) complex. Based on the elemental analysis, mass spectra, and the results from different physicochemical techniques employed in this study, a five-coordinate trigonal-bipyramidal geometry was proposed for the newly synthesized $[Cu^{II}(py^{t}BuMe_2N_3)Cl_2]$ (**1**). To confirm the proposed structure, comparative spectral and magnetic investigations were carried out with the previously prepared copper(II) complex $[Cu^{II}(py^{t}BuN_3)Cl_2]$ (**2**). The ability of **1** and **2** to oxidize 3,5-DTBC was studied and the results demonstrated that there is no correlation between the rate of chloride substitution and the observed catalytic activity. In assessing whether there is a correlation between the Lewis acidity of the central copper(II) ion and catalytic properties, no trend was observed for these complexes. Although **1** is the catalytically most active species, its Lewis acidity is lower than that of **2**. It appears that both the Lewis acidity of the central copper(II) and redox potentials are of secondary importance to chloride substitution in determining the catalytic properties of these complexes.

Acknowledgments

Kafrelsheikh University, Kafrelsheikh, Egypt, the University of Erlangen-Nuremberg, Erlangen, Germany, and the Deutsche Forschungsgemeinschaft are thanked for financial support.

References

[1] A.E. Shilov, G.B. Shul Pi. *Chem. Rev.*, **97**, 2879 (1997).
[2] B.B. Wentzel, M.P.J. Donners, P.L. Alsters, M.C. Feiters, R.J.M. Notlte. *Tetrahedron Lett.*, **56**, 7797 (2000).
[3] (a) M. Trivedi, D.S. Pandey, Q. Xu. *Inorg. Chim. Acta*, **3607**, 2492 (2007); (b) F. Calderazzo, U. Englert, G. Pampaloni, R. Santi, A. Sommazzi, M. Zinna. *Dalton Trans.*, 914 (2005).
[4] J. Scott, S. Gambarotta, I. Korobkov, Q. Knijnenburg, B. de Bruin, P.H.M. Budzelaar. *J. Am. Chem. Soc.*, **127**, 17204 (2005), and references therein.
[5] S.Y. Shaban, F.W. Heinemann, R. van Eldik. *Eur. J. Inorg. Chem.*, 3111 (2009).
[6] (a) F. Thaler, C.D. Hubbard, F.W. Heinemann, R. van Eldik, S. Schindler, I. Fabian, A.M. Dittler-Klingemann, F.E. Hahn, C. Orvig. *Inorg. Chem.*, **37**, 4022 (1998); (b) A. Company, J.-E. Jee, X. Ribas, J.M. Lopez-Valbuena, L. Gomez, M. Corbella, A. Llobet, J. Mahía, J. Benet-Buchholz, M. Costas, R. van Eldik. *Inorg. Chem.*, **46**, 9098 (2007); (c) M.M. Ibrahim, S.Y. Shaban. *Inorg. Chim. Acta*, **362**, 1471 (2009); (d) D.E. Fenton. *Chem. Soc. Rev.*, **28**, 159 (1999); (e) G.R. Cayley, I.D. Kelly, P.F. Knowles, K.D.S. Yadav. *J. Chem. Soc., Dalton Trans.*, 2370 (1981).
[7] (a) N. Wei, N.N. Murthy, Q. Chen, J. Zubieta, K.D. Karlin. *Inorg. Chem.*, **33**, 1953 (1994); (b) N. Kitajima, T. Koda, S. Hashimoto, T. Kitagawa, Y. Moro-oka. *J. Am. Chem. Soc.*, **113**, 5664 (1991).
[8] G.J.P. Britovsek, M. Bruce, V.C. Gibson, B.S. Kimberley, P.J. Maddox, S. Mastroianni, S.J. McTavish, C. Redshaw, G.A. Solan, S. Strolmberg, A.J.P. White, D.J. Williams. *J. Am. Chem. Soc.*, **121**, 8728 (1999).
[9] R. van Eldik, W. Gaede, S. Wieland, J. Kraft, M. Spitzer, D.A. Palmer. *Rev. Sci. Instrum.*, **64**, 1355 (1993).
[10] M. Spitzer, F. Gärtig, R. van Eldik. *Rev. Sci. Instrum.*, **59**, 2002 (1988).
[11] A.M. Ramadan, I.M. El-Mehasseb. *Trans. Met. Chem.*, **23**, 183 (1998), and references cited therein.
[12] K. Nakamoto. *Infrared and Raman Spectra of Inorganic and Coordination Compounds*, Wiley, New York (1986).
[13] (a) B.P. Lever, *Inorganic Electronic Spectroscopy*, Elsevier, Amsterdam (1968); (b) C.J. Ballhausen, H.B. Gray. *Inorg. Chem.*, **1**, 111 (1962).
[14] (a) D.X. West, A.A. Nassar, F.A. EI-Saied, M.I. Ayad. *Trans. Met. Chem.*, **23**, 321 (1998).

[15] E.R. Brown, R.F. Large. In *Techniques of Chemistry: Physical Methods of Chemistry*, A. Weissberger, B. Rossiter (Eds), Part IIA, Vol. 1, p. 475, Wiley, New York (1971).
[16] K.D. Karlin, P.L. Dahlstrom, J.R. Hyde, J. Zubieta. *J. Chem. Soc., Chem. Commun*., 906 (1980).
[17] A. Hofmann, D. Jaganyi, O.Q. Munro, G. Liehr, R. van Eldik. *Inorg. Chem*., **42**, 1688 (2003).
[18] B.L. Small, M. Brookhart. *Macromolecules*, **32**, 2120 (1999).
[19] (a) R. van Eldik. *Coord. Chem. Rev*., **251**, 1649 (2007); (b) J. Burgess, *Metal Ions in Solution*, Ellis Horwood, Chichester (1978); (c) C.H. Langford, H.B. Gray, *Ligand Substitution Processes*, W.A. Benjamin, p. 8 New York and Amsterdam (1965); (d) T.W. Swaddle. *Coord. Chem. Rev*., **14**, 217 (1974).
[20] J. Reim, B. Krebs. *J. Chem. Soc., Dalton Trans*., 3793 (1997).
[21] M.R. Malachowski, H.B. Huynh, L.J. Tomlinson, R.S. Kelly, J.W. Furbeejun. *J. Chem. Soc., Dalton Trans*., 31 (1995).
[22] M.R. Malachowski, B. Dorsey, J.G. Sackett, R.S. Kelly, A.L. Fekro, R.N. Hardin. *Inorg. Chim. Acta*, **249**, 85 (1996).
[23] M.R. Malachowski, M.G. Davidson, J.N. Hoffman. *Inorg. Chim. Acta*, **157**, 91 (1989).
[24] M.M. Rogic, M.D. Swerdloff, T.R. Demmin, K.D. Karlin, J. Zubieta (Eds), *Copper Coordination Chemistry: Biochemical and Inorganic Perspectives*, p. 167, Adenine Guilderland, NY (1983).